

Determination of the sticking probability of hydrocarbons on an amorphous hydrocarbon surface

12th International Workshop on Plasma Facing Materials and Components for Fusion Applications

K. Tichmann, U. von Toussaint, T. Schwarz-Selinger, W. Jacob

Max Planck Institut für Plasmaphysik,

Euratom Association; 85748 Garching, Germany

Abstract

The surface reactions of different energetic CH_y molecules were studied using classical molecular dynamics. The sticking coefficient and the sputter yield of the different hydrocarbon species were studied for kinetic energies from 5 to 100 eV. Their dependence on the energy of the projectile and the angle of incidence are reported. Additionally, the results are compared to results from TRIM calculations on a similar system.

I. INTRODUCTION

Retained tritium in redeposited layers on the walls is a serious safety concern for ITER. However, the predictions about the number of discharges after which the limit for retained fuel is exceeded are highly uncertain [1]. The total amount of tritium retained in redeposited films is to a certain extent determined by the sticking probability of hydrocarbon species impinging on the surface. Experimental data on this subject is available only for energies above 200eV [2]. The range below is investigated here using classical molecular dynamics (MD) simulations. These simulations are limited to energies below about 100 eV by the size of the sample, since at larger energies border effects can occur. At these higher energies, effects caused by the molecular nature of the projectile should diminish, so that well established programs such as TRIM [3] can take over. To assess to what extent the assumptions of the different approaches are justified, a comparison is made between the molecular dynamics simulations and TRIM calculations for a similar system.

Similar MD simulations have been done in [4, 5], but comparison is difficult due to the fact that different samples and analysis methods were used.

II. SIMULATION METHOD

The simulations were carried out with the HCparcas code [6]. This code solves the classical equations of motion of all atoms in the simulation using the Brenner hydrocarbon interaction potential [7] to account for all quantum mechanical effects. In the limit of very low flux, the sample is initially in equilibrium and individual impacts do not affect each other. This limit can be simulated by bombarding the undisturbed sample multiple times with random starting conditions. For this operation, a sample that represents the steady state for layer growth is required. Such a sample was produced by randomly putting carbon and hydrogen atoms in a box with periodic boundary conditions and then going through multiple cycles of heating the sample to 3000 K and cooling down to 200 K. Then, the periodic boundary conditions were lifted in z -direction and the sample was slowly heated to 300 K. Finally, the sample was left alone for about 300 ns to reach an equilibrium state. The result is a sample of 592 carbon and 394 hydrogen atoms, 28 Å high and 14×14 Å wide, that corresponds to a hard amorphous hydrocarbon film [8]. This sample has been

used previously to investigate chemical sputtering by simultaneous bombardment with Ar ions and thermal H atoms [9].

To avoid transferring momentum from the projectiles to the sample, the lower 2 Å of the sample were kept at fixed positions so that the sample could not drift away.

The projectile molecules were equilibrated separately and cooled down to 1 K. By cooling them to this low temperature, it can be safely assumed that the atoms are in their equilibrium positions. For any reasonable temperature of the projectile, the kinetic energy of the projectile exceeds the thermal energy of the individual atoms by more than an order of magnitude, so the extremely low projectile temperature should not affect the results of the simulation.

For bombardment, the projectile was randomly oriented and placed at a random position 15 Å above the surface. The energy of the projectile, and its angle of incidence (measured relative to the surface normal) were set to a fixed value. For each combination of projectile type, projectile kinetic energy and angle of incidence, 1000 simulation runs were performed.

III. ANALYSIS OF THE RESULTS

The sticking coefficient is defined as the probability that the carbon atom from the projectile does not leave the sample. It is determined by counting the number of *projectile* atoms that are within 1 Å above the original sample surface at the end of the simulation. The sputter yield is determined by counting the number of *sample* atoms that lie outside this region.

The simplest way to obtain a value for the sticking coefficient from this is to calculate the mean value and standard deviation of this data set. However, this approach can yield misleading results. Taking a simple example where the the number of sticking atoms were counted in ten experiments: $d = \{0, 0, 0, 0, 0, 1, 0, 0, 0, 0\}$. According to the simple calculation, a sticking coefficient $S = 0.1 \pm 0.1$ would result. Assuming a normal error distribution, this would mean that there is a probability of about 16% that the sticking coefficient is negative, which can obviously not be the case.

The reason for this behaviour is, that by calculating the mean value, it is implicitly assumed that the data comes from a Gaussian distribution, which cannot be the case here, since the data values can only assume non-negative integer values. To correctly assess this,

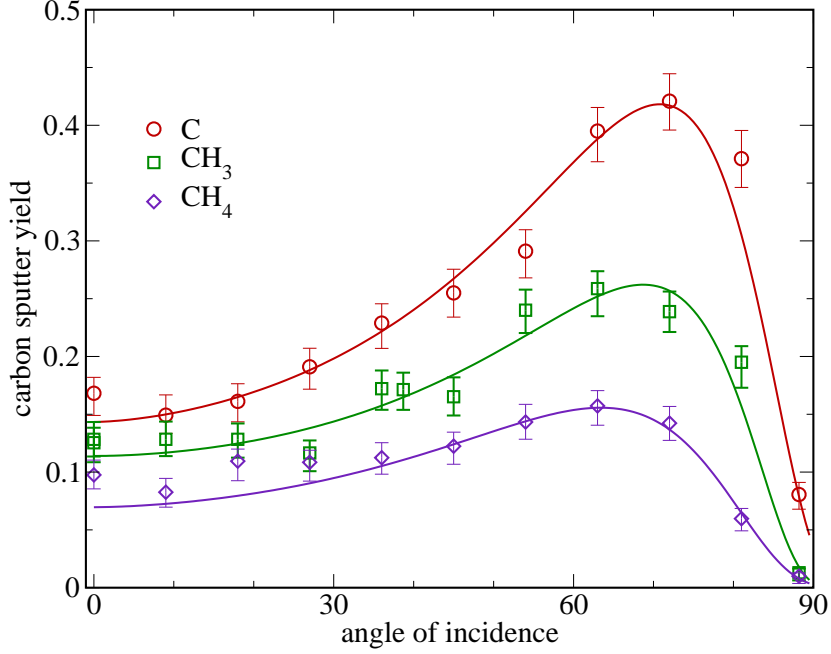


FIG. 1: Angular dependence of sputter yields for selected species at 50 eV. The results of the combined angle and energy fit to Eckstein's formula [11] are plotted as solid lines.

a multinomial distribution is used

$$p(\vec{n}|\vec{p}) = \frac{\sum_i n_i! \prod_i p_i^{n_i}}{\prod_i n_i!}, \quad (1)$$

where p_i is the probability to count i atoms in an experiment and n_i is the number of times that i atoms were counted. The mean number of counted atoms is then calculated as $\sum_i p_i i$. To calculate this number, the p_i must be determined. Nothing is known a priori about \vec{p} except that $\sum p_i = 1$. This can be expressed as a Dirichlet distribution[10] with all parameters set to 1. The posterior probability that the p_i assume particular values given the results from the simulation is then also given by a Dirichlet distribution with parameters n_i+1 from which the mean value and the statistical deviations of the final results are derived.

IV. RESULTS AND DISCUSSION

Figure 1 shows the angular dependence of the sputter yield for three different projectiles (C, CH₃, CH₄) at a kinetic energy of 50 eV. All 3 curves increase with increasing angle of incidence, show a distinct maximum at about 70° and decrease to almost zero at the

	q	ε_L	E_{th}	λ	μ	f	b	c	E_{sp}
C	1.92	5.21e-04	5.50e-02	4.66	5.06e-01	3.05	1.16	0.833	2.76e-02
CH ₃	1.90	7.18e-04	9.67e-01	6.24	7.83e-01	2.99	1.27	0.924	2.84e-01
CH ₄	3.29	6.16e-05	1.69e+00	10.01	1.47e+00	4.19	2.11	0.864	4.28e-01

TABLE I: Best fit parameters for sputtering

maximum angle of 88° where the projectiles move almost parallel to the surface. The sputter yield decreases with increasing number of hydrogen atoms in the projectile.

The data was fitted to Eckstein's fit formulae for sputter yields as function of energy or angle of incidence [11]:

$$Y(E_0, \alpha) = Y(E_0, 0) \left\{ \cos \left[\left(\frac{\alpha}{\alpha_0} \frac{\pi}{2} \right)^c \right] \right\}^{-f}$$

$$\times \exp \left\{ b \left(1 - 1 / \cos \left[\left(\frac{\alpha}{\alpha_0} \frac{\pi}{2} \right)^c \right] \right) \right\}$$

$$Y(E_0) = q s_n^{\text{KrC}} \frac{\left(\frac{E_0}{E_{\text{th}}} - 1 \right)^\mu}{\lambda/w + \left(\frac{E_0}{E_{\text{th}}} - 1 \right)^\mu}$$

with

$$\alpha_0 = \pi - \arccos \sqrt{\frac{1}{1 + E_0/E_{\text{sp}}}}$$

$$s_n^{\text{KrC}} = \frac{1}{2} \frac{\log(1 + 1.2288\varepsilon)}{w}$$

$$w = \varepsilon + 0.1728\sqrt{\varepsilon} + 0.008\varepsilon^{0.1504}$$

$$\varepsilon = \varepsilon_L E_0$$

The lines in the plot show the fit, fitted to the complete data set as a function of angle and energy, produced by multiplying Eckstein's functions for energy and angle of incidence.

The energy dependence of the sputter yield at perpendicular incidence is displayed in figure 2 for the same species. The sputter yields raise monotonously over the studied range and flattening of the curve is visible at high energies. The solid lines in the figure show the result of the fit to Eckstein's formula. Better agreement with the data can be reached if only the displayed data is fitted as function of energy only (dotted lines).

In figure 3, the sticking probability for selected species at 50 eV is plotted versus the angle of incidence. The sticking coefficient is around unity for small angles versus the surface normal and goes to zero for large angles. The sticking probability decreases for

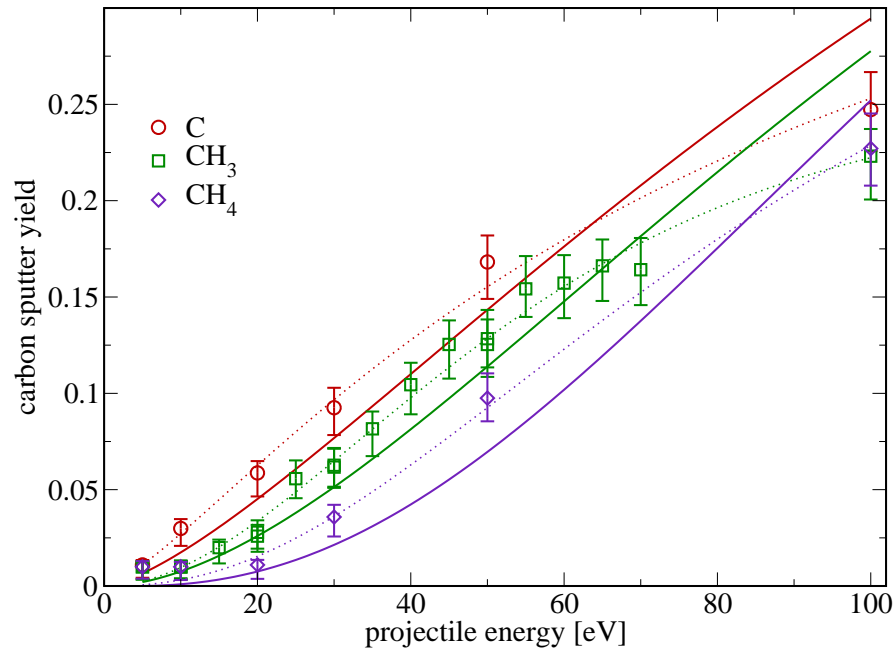


FIG. 2: Energy dependence of sputter yields for perpendicular incidence. The solid lines represent the combined angle and energy fit to Eckstein's fit formula [11], the dotted lines are energy-only fits

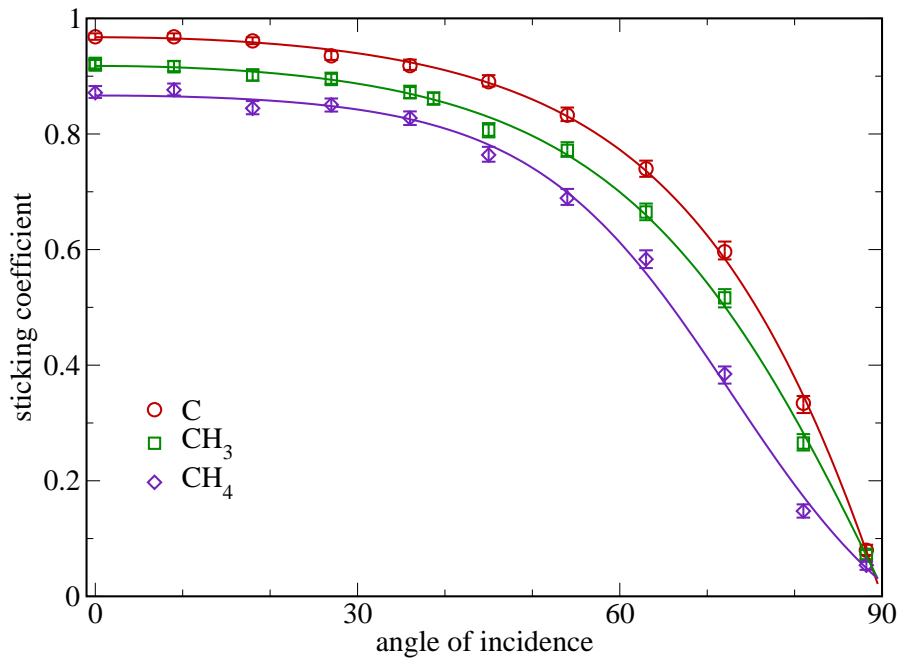


FIG. 3: Sticking coefficient of selected species at 50 eV versus their angle of incidence. The results from the fit formula (2) are plotted as solid lines.

Projectile	E	a	b	c	d
C	50	1.947	2.104	0.843	-0.923
CH ₃	50	1.015	1.798	0.980	-0.043
CH ₄	50	0.534	1.962	1.238	0.353

TABLE II: Fit parameters for angular dependence of sticking coefficient

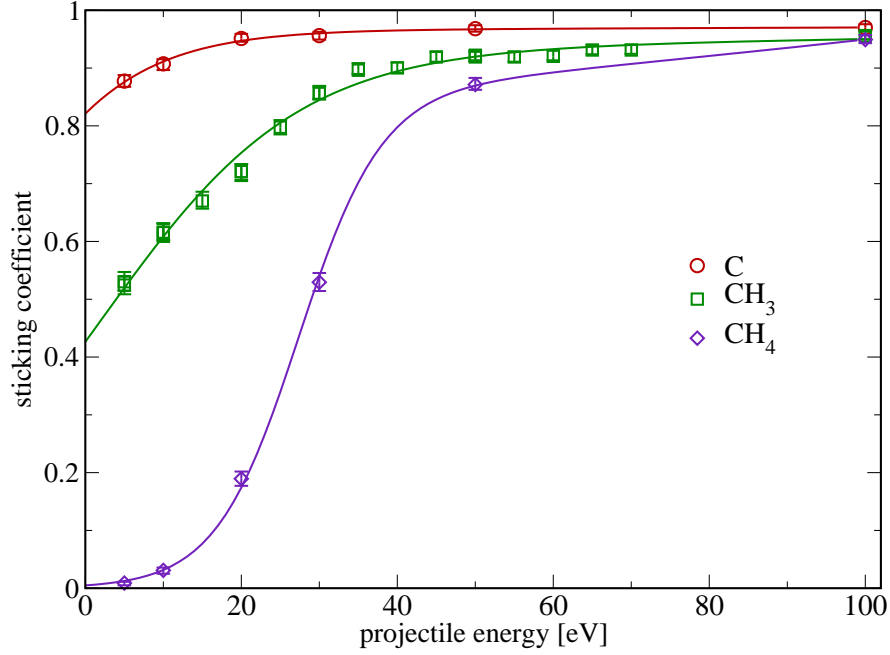


FIG. 4: Energy dependence of sticking coefficient for perpendicular incidence together with the results of fit formula (3) as solid lines

larger numbers of hydrogen atoms in the projectile, probably resulting from the fact that the projectiles with less hydrogen have a higher reactivity. Since no suitable fit formula could be found to describe the data, a new one was developed from a cosine-like function that saturates for small angles:

$$S(\alpha) = a \cdot \tanh(b \cdot \cos(c\alpha)) + d \quad (2)$$

This formula has no physical background and can thus only be used to interpolate the data. The results from the fit of this formula to the data are shown in figure 3 as solid lines.

Figure IV depicts the data of selected species for perpendicular incidence as a function of energy together with the associated fit functions plotted as lines. At the low energy end, a

Projectile θ	a	b	c	d
C -0	1.74	1.076e-01	-4.984e-05	0.965
CH ₃ -0	-0.17	7.989e-02	-2.209e-04	0.929
CH ₄ -0	-5.11	1.882e-01	-1.336e-03	0.823

TABLE III: Fit parameters for energy dependence of sticking coefficient

threshold behaviour is visible for CH₄. This suggests that a certain activation energy must be provided to chemisorb CH₄.

Comparing the data to similar simulations in [5], the sticking is lower by about one third, showing the same trend. A more quantitative comparison of the sticking coefficients is complicated by the fact that the sample used in [5] is not an amorphous one.

For high energies, all sticking coefficients approach 1. This does not necessarily mean that the layer grows, since the sputtering also increases for higher energy. While sticking strongly depends on the projectile species at low energies, the effect diminishes for higher energies with almost no difference at 100 eV. To fit the threshold behaviour of the sticking coefficient, a sigmoidal function with some additions to correct the high energy side was used:

$$S(E) = \frac{1}{1 + \exp(-a - b \cdot E)} \frac{c}{1 + d \cdot E}. \quad (3)$$

Again, this formula was created without physical background.

For higher energies, programs based on the binary collision approximation like TRIM [3] are commonly used. They do not take into account the chemical bonding of the sample and do not model the molecular nature of the projectile at all. Since the kinetic energy of the projectile eventually dominates the chemical binding energy, the influence of the molecular structure of the projectile vanishes with increasing energy. To study to what extent the results of the molecular dynamics simulations differ from the well-established TRIM calculations, a similar system was modelled in SDTrim.SP [12] using a surface binding energy of 2.8 eV [13]. The results of the calculations for the energy dependence of sticking and sputtering of CH₃ at a fixed angle of incidence of 38° are plotted as lines in figure 5. TRIM calculations are orders of magnitude faster than MD calculations, so much better statistics and resolution can be achieved. As can be seen from figure 5, the sputtering yields show the same thresholding behaviour, but the absolute value of the sputtering yield is

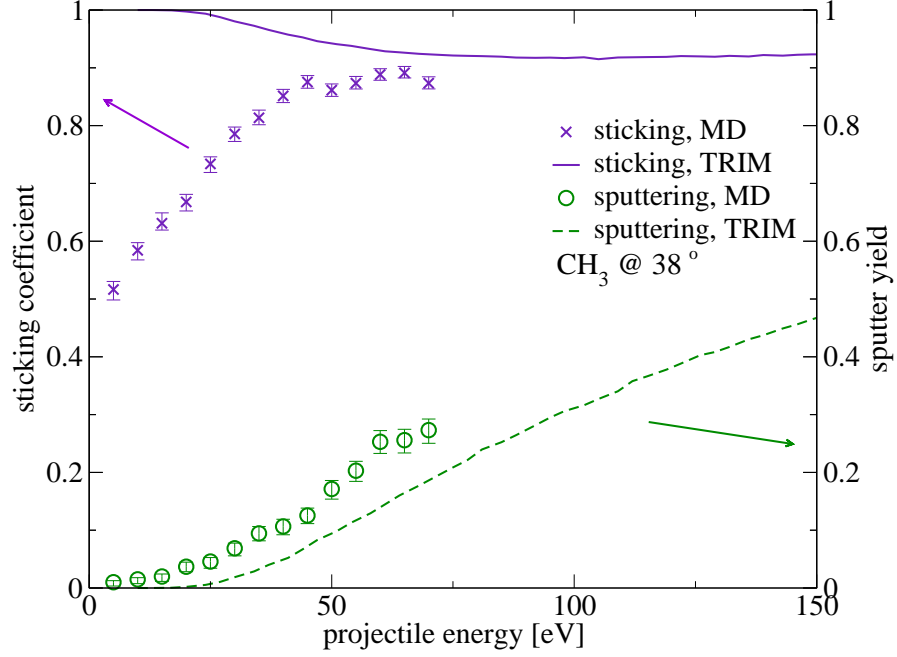


FIG. 5: Sputtering yields and sticking coefficients from MD (symbols) and TRIM (lines), calculated for CH_3 at 38°

about a factor of 2 lower with TRIM. This might be explained by the fact that the TRIM calculations do not model surface roughness or binding energy distributions and the sample composition is slightly different, although any of these points could also affect the result in the opposite direction. The sticking however, shows a completely different behaviour for low energies. While the MD simulated sticking decreases from about 0.9 to about 0.5, the TRIM calculated value increases to 1 for low energies. In this region, the behaviour of TRIM is dominated by the parameter value of surface binding energy. This parameter does not properly reflect the actual physical properties relevant for sticking. For high energies, the sticking coefficients determined by MD and TRIM approach the same value.

V. CONCLUSION

Results from classical molecular dynamics simulations of hydrocarbon molecules and fragments impinging on a amorphous hydrocarbon sample were presented. The resulting sputter yields can be fitted using Eckstein's Fit formulae [11], allowing to compress the simulation results into a simple formula of energy and angle of incidence. For the sticking

probability, a new fit formula is proposed that facilitates the compression and interpolation of the MD data.

While the absolute sputtering yields of the TRIM and molecular dynamics simulation results not unexpectedly differ in the low energy range where the assumptions of the TRIM simulations are no longer valid, the threshold behaviour is the same for both methods of calculation. At high energies, the MD results for different projectile molecule species converge, since the molecular binding energy becomes negligible against the kinetic energy of the projectile. The sticking coefficients of TRIM and MD approach the same value for high energies, but in the low energy range TRIM shows an unphysical behaviour that is not reproduced by MD simulations.

Bibliography

- [1] J. Roth, A. Kirschner, W. Bohmeyer, S. Brezinsek, A. Cambe, E. Casarotto, R. Doerner, E. Gauthier, G. Federici, S. Higashijima, J. Hogan, A. Kallenbach, H. Kubo, J.M. Layet, T. Nakano, V. Philipps, A. Pospieszczyk, R. Preuss, R. Pugno, R. Ruggiéri, B. Schweer, G. Sergienko, and M. Stamp. Flux dependence of carbon erosion and implication for iter. *Journal of Nuclear Materials*, 337-339:970 – 974, 2005. PSI-16.
- [2] Wenmin Wang, J. Roth, W. Eckstein, R. Schwoerer, H. Plank, and Maohua Du. Deposition of amorphous hydrogenated carbon films due to hydrocarbon molecule ion-beam bombardment. *Nuclear Instruments and Methods in Physics Research Section B: Beam Interactions with Materials and Atoms*, 129(2):210 – 216, 1997.
- [3] J. P. Biersack and W. Eckstein. Sputtering studies with the monte carlo program trim.sp. *Applied Physics A: Materials Science & Processing*, 34(2):73–94, 06 1984.
- [4] A.R. Sharma, R. Schneider, U. Toussaint, and K. Nordlund. Hydrocarbon radicals interaction with amorphous carbon surfaces. *Journal of Nuclear Materials*, 363-365:1283 – 1288, 2007. Plasma-Surface Interactions-17.
- [5] D A Alman and D N Ruzic. Molecular dynamics simulation of hydrocarbon reflection and dissociation coefficients from fusion-relevant carbon surfaces. *Physica Scripta*, T111:145–151,

2004.

- [6] K. Nordlund, J. Keinonen, and T. Mattila. Formation of ion irradiation induced small-scale defects on graphite surfaces. *Phys. Rev. Lett.*, 77(4):699–702, Jul 1996.
- [7] Donald W. Brenner. Empirical potential for hydrocarbons for use in simulating the chemical vapor deposition of diamond films. *Phys. Rev. B*, 42(15):9458–9471, Nov 1990.
- [8] T. Schwarz-Selinger, A. von Keudell, and W. Jacob. Plasma chemical vapor deposition of hydrocarbon films: The influence of hydrocarbon source gas on the film properties. *Journal of Applied Physics*, 86(7):3988–3996, 1999.
- [9] P N Maya, U von Toussaint, and C Hopf. Synergistic erosion process of hydrocarbon films: a molecular dynamics study. *New Journal of Physics*, 10(2):023002 (15pp), 2008.
- [10] Luc Devroye. *Non-Uniform Random Variate Generation*. Springer, 1986.
- [11] W. Eckstein and R. Preuss. New fit formulae for the sputtering yield. *Journal of Nuclear Materials*, 320(3):209 – 213, 2003.
- [12] Valentin Stierle. Bestimmung der Streu- und Haftungskoeffizienten von Kohlenwasserstoffmolekülen auf a-C:H Schichten durch TRIM-Simulation. Bachelor thesis, Ludwig-Maximilians-Universität München, 2009.
- [13] W Jacob, C Hopf, and M Schluter. Chemical sputtering of carbon materials due to combined bombardment by ions and atomic hydrogen. *Physica Scripta*, T124:32–36, 2006.